Space-Time and Space-Frequency Block Coded Vector OFDM Modulation

Jing Han, *Member, IEEE,* and Geert Leus, *Fellow, IEEE*

***Abstract*—Vector orthogonal frequency division multiplexing (OFDM) is a promising modulation scheme which allows for a flexible configuration and connects OFDM and single-carrier frequency domain equalization (SC-FDE) in a unified framework. In this letter, we design Alamouti-like space-time block coded (STBC) and space-frequency block coded (SFBC) vector OFDM systems. Based on these schemes, we prove that, with two transmit and one receive antenna, the diversity order of the zero-forcing (ZF) receiver is fixed to 2 over frequency selective fading channels, while that of the minimum mean square error (MMSE) receiver depends on the channel memory length, the vector block (VB) size and the spectral efficiency.**

***Index Terms*—Vector OFDM, space-time block coding (STBC), space-frequency block coding (SFBC), diversity order.**

I. INTRODUCTION

CURRENTLY, orthogonal frequency division multiplexing (OFDM) and single-carrier frequency domain equalization (SC-FDE) are two primary techniques widely adopted in wireless systems. Although both schemes have the merit of low complexity based on frequency-domain processing, each one has its relative drawbacks. Specifically, OFDM suffers from the well-known large peak-to-average power ratio (PAPR) and high sensitivity to carrier frequency offset, while SC-FDE leads to an unbalanced complexity in the transceiver as well as an inflexible bandwidth and energy management.

To solve this problem, a generalized modulation scheme named vector OFDM (V-OFDM), which was first proposed in [1], has seen a revival. By introducing the so-called vector block (VB), V-OFDM provides a unified framework to trade off resource management flexibility with PAPR, and thus bridges the gap between OFDM and SC-FDE. Moreover, its system performance is analyzed based on maximum likelihood (ML) and linear receivers [2], [3].

So far, most V-OFDM research focuses on configurations with a single transmit antenna. To the best of our knowledge, the cyclic delay diversity (CDD) V-OFDM scheme in [4] is the first attempt on a multiple-antenna extension. In this letter, we alternatively propose two Alamouti-like schemes, namely, space-time block coded (STBC) and space-frequency block coded (SFBC) V-OFDM, to collect diversity in the spatial domain. The main contributions are listed as follows.

- The proposed V-OFDM schemes operate on a VB basis aided by a vector-specific phase rotation. Each of them yields a generalized framework, which incorporates the existing Alamouti-like OFDM and SC-FDE systems as special cases.
- Linear receivers based on zero-forcing (ZF) and minimum mean square error (MMSE) criteria are presented in the frequency domain. Moreover, a theoretical diversity order analysis is performed, which reveals that, with two transmit and one receive antenna, the diversity order of the ZF receiver is fixed to $d_{\text{ZF}} = 2$ over frequency selective fading channels. In contrast, for the MMSE receiver, we obtain the diversity order $d_{\text{MMSE}} = 2\left(\min\left\{\lfloor M2^{-R}\rfloor, D\right\}+1\right)$, where $\lfloor\cdot\rfloor$ denotes the integer floor operation. D, M and R are the channel memory length, VB size and spectral efficiency, respectively.

Notation: $(\cdot)^*$ stands for conjugate, $(\cdot)^T$ for transpose, $(\cdot)^H$ for Hermitian transpose and $\text{Tr}\{\cdot\}$ for trace. $\otimes$ represents the Kronecker product. We define $[\mathbf{a}]_n$ as the n-th entry of the vector $\mathbf{a}$, $\text{diag}\{\mathbf{x}\}$ as a diagonal matrix created from the vector $\mathbf{x}$, and $\text{Diag}\{\mathbf{A}_1,\dots,\mathbf{A}_M\}$ as a block diagonal matrix created with the submatrices $\mathbf{A}_1,\dots,\mathbf{A}_M$. $\mathbf{1}_{M\times N}$ and $\mathbf{0}_{M\times N}$ denote the $M\times N$ all-one and all-zero matrices. $\mathbf{F}_M$, $\mathbf{I}_M$ and $\mathbf{P}_M$ are the $M\times M$ unitary DFT, identity and permutation matrix satisfying $[\mathbf{P}_M\mathbf{a}]_m = [\mathbf{a}]_{(-m)\bmod M}$, respectively.

II. STBC AND SFBC V-OFDM

The STBC and SFBC V-OFDM system structure is shown in Fig. 1. We consider a scenario with two transmit and one receive antenna. At the transmitter, each data block of $N = ML$ symbols with mean zero and variance σ_x^2 is first partitioned into L transmit VBs, i.e.,

$$\mathbf{x}_k \triangleq \left[\mathbf{x}_{k,0}^T, \mathbf{x}_{k,1}^T, \dots, \mathbf{x}_{k,L-1}^T\right]^T, \tag{1}$$

where k is the block index and $\{\mathbf{x}_{k,l}\}_{l=0}^{L-1}$ are the length-M VBs. Then, at each transmit antenna $\mu \in \{1,2\}$, the space-time or space-frequency encoding is performed on a VB basis, from which the coded VBs $\{\bar{\mathbf{x}}_{k,l}^{(\mu)}\}$ are obtained. Using a size-L vector IDFT, the signal forwarded to the antenna μ is

$$\mathbf{s}_k^{(\mu)} = \left[\mathbf{F}_L^H \otimes \mathbf{I}_M\right]\bar{\mathbf{x}}_k^{(\mu)}, \tag{2}$$

Manuscript received xxxx xx, 2016; revised xxxx xx, 2016; accepted xxxx xx, 2016. Date of publication xxxx xx, 2016; date of current version xxxx xx, 2016. This work was supported by National Natural Science Foundation of China under Grant 61001153, 61401499 and 61501374, Fundamental Research Funds for the Central Universities under Grant 3102014JCQ01010, 3102014ZD0041, and Natural Science Basic Research Plan in Shaanxi Province of China under Grant 2015JQ6220. The associate editor coordinating the review of this letter and approving it for publication was T. Riihonen.

J. Han is with the School of Marine Science and Technology, Northwestern Polytechnical University, Xi'an 710072, China (e-mail: hanj@nwpu.edu.cn).

G. Leus is with the Faculty of Electrical Engineering, Mathematics and Computer Science, Delft University of Technology, 2826 CD Delft, The Netherlands (e-mail: g.j.t.leus@tudelft.nl).

Digital Object Identifier 10.1109/LCOMM.2016.xxxxxxx

This article has been accepted for publication in a future issue of this journal, but has not been fully edited. Content may change prior to final publication. Citation information: DOI 10.1109/LCOMM.2016.2614812, IEEE Communications Letters

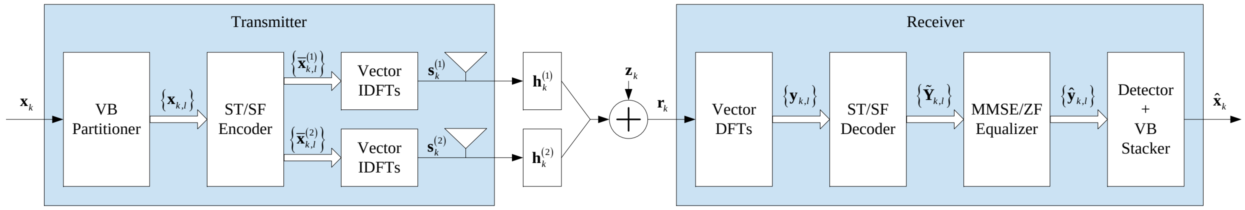

Fig. 1. Structure of the STBC and SFBC V-OFDM communication systems.

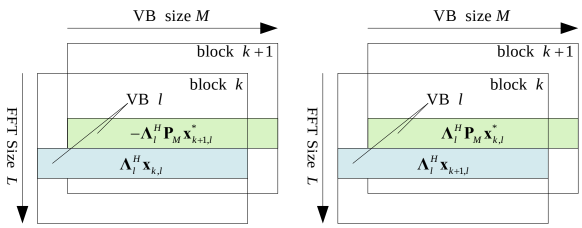

(a) Antenna 1 (b) Antenna 2

Fig. 2. STBC V-OFDM transmit block format.

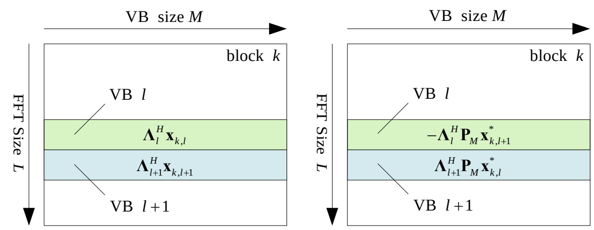

(a) Antenna 1 (b) Antenna 2

Fig. 3. SFBC V-OFDM transmit block format.

where $\bar{\mathbf{x}}_k^{(\mu)} \triangleq [\bar{\mathbf{x}}_{k,0}^{(\mu)T}, \bar{\mathbf{x}}_{k,1}^{(\mu)T}, \ldots, \bar{\mathbf{x}}_{k,L-1}^{(\mu)T}]^T$. Finally, a cyclic prefix (CP) is inserted and the resulting signal is transmitted through the μ-th channel, which is assumed to be frequency-selective over block k and is modeled by the $(D+1) \times 1$ impulse response vector $\mathbf{h}_k^{(\mu)} \triangleq [h_{k,0}^{(\mu)}, h_{k,1}^{(\mu)}, \ldots, h_{k,D}^{(\mu)}]^T$.

At the receiver, after removing the CP, the baseband received signal can be expressed as

$$\mathbf{r}_k = \mathbf{H}_k^{(1)}\mathbf{s}_k^{(1)} + \mathbf{H}_k^{(2)}\mathbf{s}_k^{(2)} + \mathbf{z}_k, \tag{3}$$

where $\mathbf{z}_k \sim \mathcal{CN}(\mathbf{0}, \sigma_z^2\mathbf{I}_N)$ is the complex Gaussian noise vector, $\mathbf{H}_k^{(\mu)}$ is the $N \times N$ circulant channel matrix with first column equal to $\mathbf{h}_k^{(\mu)}$ appended by $N-D-1$ zeros. Using a size-L vector DFT, we have

$$\mathbf{y}_k = [\mathbf{F}_L \otimes \mathbf{I}_M]\,\mathbf{r}_k, \tag{4}$$

where $\mathbf{y}_k \triangleq [\mathbf{y}_{k,0}^T, \mathbf{y}_{k,1}^T, \ldots, \mathbf{y}_{k,L-1}^T]^T$, and $\mathbf{y}_{k,l}$ is the l-th receive VB of the form

$$\mathbf{y}_{k,l} = \mathbf{U}_l^H \bar{\mathbf{H}}_{k,l}^{(1)} \mathbf{U}_l \bar{\mathbf{x}}_{k,l}^{(1)} + \mathbf{U}_l^H \bar{\mathbf{H}}_{k,l}^{(2)} \mathbf{U}_l \bar{\mathbf{x}}_{k,l}^{(2)} + \mathbf{z}_{k,l}, \tag{5}$$

where $\bar{\mathbf{H}}_{k,l}^{(\mu)} \triangleq \mathrm{diag}\left\{\left[H_{k,l}^{(\mu)}, H_{k,l+L}^{(\mu)}, \ldots, H_{k,l+(M-1)L}^{(\mu)}\right]\right\}$ is the channel matrix with entries $H_{k,n}^{(\mu)} = \sum_{d=0}^{D} h_{k,d}^{(\mu)} e^{-j\frac{2\pi dn}{N}}$, $\mathbf{U}_l = \mathbf{F}_M \boldsymbol{\Lambda}_l$ and $\boldsymbol{\Lambda}_l \triangleq \mathrm{diag}\left\{\left[1, e^{-j\frac{2\pi l}{N}}, \ldots, e^{-j\frac{2\pi(M-1)l}{N}}\right]\right\}$. $\mathbf{z}_{k,l}$ is the noise vector. In order to decouple the VBs in (5), STBC and SFBC V-OFDM schemes are detailed as follows.

A. STBC V-OFDM Scheme

Our STBC V-OFDM scheme is depicted in Fig. 2, where the encoder generates the coded VBs

$$\begin{bmatrix} \bar{\mathbf{x}}_{k,l}^{(1)} & \bar{\mathbf{x}}_{k+1,l}^{(1)} \\ \bar{\mathbf{x}}_{k,l}^{(2)} & \bar{\mathbf{x}}_{k+1,l}^{(2)} \end{bmatrix} = \begin{bmatrix} \boldsymbol{\Lambda}_l^H \mathbf{x}_{k,l} & -\boldsymbol{\Lambda}_l^H \mathbf{P}_M \mathbf{x}_{k+1,l}^* \\ \boldsymbol{\Lambda}_l^H \mathbf{x}_{k+1,l} & \boldsymbol{\Lambda}_l^H \mathbf{P}_M \mathbf{x}_{k,l}^* \end{bmatrix}, \tag{6}$$

for $l = 0, 1, \ldots, L-1$. It is assumed that the channels are fixed over two consecutive blocks, i.e., $\bar{\mathbf{H}}_{k,l}^{(\mu)} = \bar{\mathbf{H}}_{k+1,l}^{(\mu)} = \bar{\mathbf{H}}_l^{(\mu)}$, $\mu \in \{1, 2\}$. Then, by substituting (6) into (5) and defining $\mathbf{X}_{k,l} = \mathbf{F}_M \mathbf{x}_{k,l}$, $\bar{\mathbf{Y}}_{k,l} = \mathbf{U}_l \mathbf{y}_{k,l}$ and $\bar{\mathbf{Z}}_{k,l} = \mathbf{U}_l \mathbf{z}_{k,l}$, we have

$$\begin{aligned}\bar{\mathbf{Y}}_l \triangleq \begin{bmatrix} \bar{\mathbf{Y}}_{k,l} \\ \bar{\mathbf{Y}}_{k+1,l}^* \end{bmatrix} &= \begin{bmatrix} \bar{\mathbf{H}}_l^{(1)} & \bar{\mathbf{H}}_l^{(2)} \\ \bar{\mathbf{H}}_l^{(2)*} & -\bar{\mathbf{H}}_l^{(1)*} \end{bmatrix} \begin{bmatrix} \mathbf{X}_{k,l} \\ \mathbf{X}_{k+1,l} \end{bmatrix} + \begin{bmatrix} \bar{\mathbf{Z}}_{k,l} \\ \bar{\mathbf{Z}}_{k+1,l}^* \end{bmatrix} \\ &\triangleq \boldsymbol{\Gamma}_l \mathbf{X}_l + \bar{\mathbf{Z}}_l, \end{aligned} \tag{7}$$

which can be further transformed as $\tilde{\mathbf{Y}}_l = \boldsymbol{\Gamma}_l^H \bar{\mathbf{Y}}_l$, i.e.,

$$\tilde{\mathbf{Y}}_l \triangleq \begin{bmatrix} \tilde{\mathbf{Y}}_{k,l} \\ \tilde{\mathbf{Y}}_{k+1,l} \end{bmatrix} = \begin{bmatrix} \tilde{\mathbf{H}}_l & \mathbf{0} \\ \mathbf{0} & \tilde{\mathbf{H}}_l \end{bmatrix} \begin{bmatrix} \mathbf{X}_{k,l} \\ \mathbf{X}_{k+1,l} \end{bmatrix} + \begin{bmatrix} \tilde{\mathbf{Z}}_{k,l} \\ \tilde{\mathbf{Z}}_{k+1,l} \end{bmatrix}, \tag{8}$$

where $\tilde{\mathbf{H}}_l = \bar{\mathbf{H}}_l^{(1)H}\bar{\mathbf{H}}_l^{(1)} + \bar{\mathbf{H}}_l^{(2)H}\bar{\mathbf{H}}_l^{(2)}$; $\tilde{\mathbf{Z}}_{k,l}$ and $\tilde{\mathbf{Z}}_{k+1,l}$ are noise terms with auto-correlation matrix equal to $\sigma_n^2 \tilde{\mathbf{H}}_l$.

B. SFBC V-OFDM Scheme

Similarly, our SFBC V-OFDM scheme is depicted in Fig. 3, where the encoder generates the coded VBs

$$\begin{bmatrix} \bar{\mathbf{x}}_{k,l}^{(1)} & \bar{\mathbf{x}}_{k,l+1}^{(1)} \\ \bar{\mathbf{x}}_{k,l}^{(2)} & \bar{\mathbf{x}}_{k,l+1}^{(2)} \end{bmatrix} = \begin{bmatrix} \boldsymbol{\Lambda}_l^H \mathbf{x}_{k,l} & \boldsymbol{\Lambda}_{l+1}^H \mathbf{x}_{k,l+1} \\ -\boldsymbol{\Lambda}_l^H \mathbf{P}_M \mathbf{x}_{k,l+1}^* & \boldsymbol{\Lambda}_{l+1}^H \mathbf{P}_M \mathbf{x}_{k,l}^* \end{bmatrix}, \tag{9}$$

for $l = 0, 2, \ldots, L-2$. Under the assumption that the channels are constant between adjacent VBs, i.e., $\bar{\mathbf{H}}_{k,l}^{(\mu)} = \bar{\mathbf{H}}_{k,l+1}^{(\mu)} = \bar{\mathbf{H}}_l^{(\mu)}$, $\mu \in \{1, 2\}$, by substituting (9) into (5), we get

$$\begin{aligned}\bar{\mathbf{Y}}_l' \triangleq \begin{bmatrix} \bar{\mathbf{Y}}_{k,l} \\ \bar{\mathbf{Y}}_{k,l+1}^* \end{bmatrix} &= \begin{bmatrix} \bar{\mathbf{H}}_l^{(1)} & -\bar{\mathbf{H}}_l^{(2)} \\ \bar{\mathbf{H}}_l^{(2)*} & \bar{\mathbf{H}}_l^{(1)*} \end{bmatrix} \begin{bmatrix} \mathbf{X}_{k,l} \\ \mathbf{X}_{k,l+1}^* \end{bmatrix} + \begin{bmatrix} \bar{\mathbf{Z}}_{k,l} \\ \bar{\mathbf{Z}}_{k,l+1}^* \end{bmatrix} \\ &\triangleq \boldsymbol{\Gamma}_l' \mathbf{X}_l' + \bar{\mathbf{Z}}_l', \end{aligned} \tag{10}$$

which as before can be transformed as $\tilde{\mathbf{Y}}_l' = (\boldsymbol{\Gamma}_l')^H \bar{\mathbf{Y}}_l'$, i.e.,

$$\tilde{\mathbf{Y}}_l' \triangleq \begin{bmatrix} \tilde{\mathbf{Y}}_{k,l} \\ \tilde{\mathbf{Y}}_{k,l+1} \end{bmatrix} = \begin{bmatrix} \tilde{\mathbf{H}}_l & \mathbf{0} \\ \mathbf{0} & \tilde{\mathbf{H}}_l \end{bmatrix} \begin{bmatrix} \mathbf{X}_{k,l} \\ \mathbf{X}_{k,l+1}^* \end{bmatrix} + \begin{bmatrix} \tilde{\mathbf{Z}}_{k,l} \\ \tilde{\mathbf{Z}}_{k,l+1} \end{bmatrix}. \tag{11}$$

It can be seen from (8) and (11) that, after space-time or space-frequency decoding, the transmit VBs are decoupled in a similar manner. Therefore, ZF and MMSE equalizers for each VB have the same form and are given by

$$\mathbf{W}_l^{\mathrm{ZF}} = \tilde{\mathbf{H}}_l^{-1}, \quad \mathbf{W}_l^{\mathrm{MMSE}} = \left(\tilde{\mathbf{H}}_l + \rho^{-1}\mathbf{I}_M\right)^{-1}, \tag{12}$$

where $\rho = \sigma_x^2/\sigma_z^2$ is the input signal-to-noise ratio (SNR).

Remark 1: As shown in (6) and (9), the proposed STBC and SFBC V-OFDM schemes perform coding on a VB basis, with vector-specific phase rotation matrices $\{\mathbf{\Lambda}_l^H\}$ inserted to guarantee a decoupled detection in (8) and (11).

Remark 2: It can be validated that STBC V-OFDM reduces to STBC OFDM [5] and STBC SC-FDE [6] when $M = 1$ and $M = N$, respectively. Meanwhile, SFBC V-OFDM is equivalent to SFBC OFDM [7] when $M = 1$, and SFBC SC-FDE [8] when $M = N/2$ [1].

III. Diversity Analysis

We analyze the performance of STBC and SFBC V-OFDM systems in terms of their diversity order, which is defined as

$$d \triangleq -\lim_{\rho\to\infty} \frac{\log P_{\text{err}}}{\log \rho}, \tag{13}$$

where P_{err} denotes the pairwise error probability (PEP). However, since the direct computation of (13) is not tractable, we here adopt an alterative approach proposed in [9], [10].

Specifically, we first consider STBC V-OFDM. In this case, the output VB of the equalizer is $\hat{\mathbf{y}}_{k,l} = \mathbf{F}_M^H \mathbf{W}_l \tilde{\mathbf{Y}}_{k,l}$, where $\mathbf{W}_l$ stands for $\mathbf{W}_l^{\text{ZF}}$ or $\mathbf{W}_l^{\text{MMSE}}$. Following the notation in [9], we define the outage diversity and probability as

$$d_{\text{out}} \triangleq -\lim_{\rho\to\infty} \frac{\log P_{\text{out}}}{\log \rho}, \tag{14}$$

$$P_{\text{out}} \triangleq \mathbb{P}\left\{\frac{1}{M} I\left(\mathbf{x}_{k,l}; \hat{\mathbf{y}}_{k,l}\right) < R\right\}, \tag{15}$$

where R is the spectral efficiency in bits/symbol, and $I\left(\mathbf{x}_{k,l}; \hat{\mathbf{y}}_{k,l}\right)$ is the effective mutual information between $\mathbf{x}_{k,l}$ and $\hat{\mathbf{y}}_{k,l}$. Also, we say that two functions $f(\rho)$ and $g(\rho)$ are exponentially equal, denoted as $f(\rho) \doteq g(\rho)$, if

$$\lim_{\rho\to\infty} \frac{\log f(\rho)}{\log \rho} = \lim_{\rho\to\infty} \frac{\log g(\rho)}{\log \rho}. \tag{16}$$

It has been proven in [9] that the diversity order $d = d_{\text{out}}$, i.e., P_{err} and P_{out} are exponentially equal. Moreover, the following result provided in [10] is here repeated as a lemma.

Lemma 1: Assuming $\{\tilde{\lambda}_m\}_{m=1}^M$ are independent and identically distributed (i.i.d.) Gamma random variables with shape parameter J, for a real-valued constant $i \in (0, M)$, we have

$$\mathbb{P}\left\{\sum_{m=1}^{M} \frac{1}{1+\rho\tilde{\lambda}_m} > i\right\} \doteq \rho^{-J(\lfloor i \rfloor + 1)}. \tag{17}$$

Based on this lemma, our diversity analysis of STBC V-OFDM is presented as follows.

Theorem 1: In 2×1 frequency-selective channels with i.i.d. zero-mean complex Gaussian taps, the diversity order of the STBC V-OFDM system with MMSE equalization is

$$d^{\text{MMSE}} = 2\left(\min\left\{\lfloor M2^{-R}\rfloor, D\right\} + 1\right), \tag{18}$$

where D, M and R are the channel memory length, VB size and spectral efficiency respectively.

[1]The only difference is that, when $M = N/2$, SFBC V-OFDM uses the first and second half of the block as two VBs, while SFBC SC-FDE in [8] divides the block into even and odd symbols.

Proof: Since the channels are assumed to be time-invariant, we drop the block index k here for simplicity. With this notation, for the l-th VB, the detection signal-to-interference-plus-noise ratio (SINR) of its m-th symbol is

$$\gamma_{l,m}^{\text{MMSE}} = \left[\frac{1}{M}\text{Tr}\left\{\left(\mathbf{I}_M + \rho\tilde{\mathbf{H}}_l\right)^{-1}\right\}\right]^{-1} - 1, \tag{19}$$

which does not depend on m. Consequently, we have the outage probability

$$\begin{aligned} P_{\text{out}} &= \mathbb{P}\left\{\frac{1}{M}\sum_{m=0}^{M-1}\log\left(1+\gamma_{l,m}^{\text{MMSE}}\right) < R\right\} \\ &= \mathbb{P}\left\{\sum_{m=0}^{M-1}\frac{1}{1+\rho\left|H_{mL+l}^{(1)}\right|^2+\rho\left|H_{mL+l}^{(2)}\right|^2} > \frac{M}{2^R}\right\}. \end{aligned} \tag{20}$$

Since it is easy to show that the joint probability density function (PDF) of $\{H_{mL+l}^{(\mu)} | \, \mu = 1,2;\, m = 0,\ldots,M-1\}$ is independent of l [3, Lemma 1], all VBs have identical P_{out} and thus identical diversity order d^{MMSE}.

Furthermore, to determine the specific value of d^{MMSE}, we adopt the strategy used in [3], which separately considers two cases, i.e., $M \geq D+1$ and $M < D+1$. For the former case, the analysis will be the same as that of STBC SC-FDE presented in [10] and the diversity order is obtained as

$$d^{\text{MMSE}} = \begin{cases} 2(D+1) & \text{for } R \leq \log\frac{M}{D}, \\ 2\left(\lfloor M2^{-R}\rfloor + 1\right) & \text{for } R > \log\frac{M}{D}, \end{cases} \tag{21}$$

which can also be expressed compactly as (18).

However, for the STBC V-OFDM system, there exists another possibility that $M < D+1$, which is not covered in [10]. Without loss of generality, we choose the VB $l = 0$ to simplify the derivation in this case. We define the $M\times 1$ vectors $\bar{\mathbf{h}}_l^{(\mu)}$ and $\tilde{\mathbf{h}}_l$ containing the diagonal entries of $\bar{\mathbf{H}}_l^{(\mu)}$ and $\tilde{\mathbf{H}}_l$, respectively. Then, if $D+1$ is divisible by M, i.e., $D+1 = QM$, we have $\bar{\mathbf{h}}_0^{(\mu)} = \mathbf{G}_A\mathbf{h}^{(\mu)}$, where

$$\mathbf{G}_A \triangleq \sqrt{M}\left(\mathbf{1}_{1\times Q}\otimes\mathbf{F}_M\right). \tag{22}$$

Since $\mathbf{G}_A\mathbf{G}_A^H = (D+1)\mathbf{I}_M$, the entries of $\bar{\mathbf{h}}_0^{(\mu)}$ are i.i.d. Gaussian random variables, and thus the entries of $\tilde{\mathbf{h}}_0$, i.e., $\{|H_{mL+l}^{(1)}|^2 + |H_{mL+l}^{(2)}|^2\}$ in (20) are i.i.d. Gamma variables with shape parameter $J = 2$ when $l = 0$. By recognizing $M/2^R \in (0, M)$ for $R > 0$, we invoke Lemma 1 to obtain

$$P_{\text{out}} \doteq \rho^{-2\left(\lfloor M2^{-R}\rfloor+1\right)}. \tag{23}$$

On the other hand, if $D+1 = QM+S$ and $0 < S < M$, we have $\bar{\mathbf{h}}_0^{(\mu)} = \mathbf{G}_B\mathbf{h}^{(\mu)}$ and

$$\mathbf{G}_B \triangleq \sqrt{M}\left[\left(\mathbf{1}_{1\times Q}\otimes\mathbf{F}_M\right), \mathbf{F}_M\mathbf{T}_S\right], \tag{24}$$

where $\mathbf{T}_S \triangleq \left[\mathbf{I}_S, \mathbf{0}_{S\times(M-S)}\right]^T$. In this case, $\mathbf{G}_B\mathbf{G}_B^H = \mathbf{F}_M\mathbf{\Sigma}\mathbf{F}_M^H$ and $\mathbf{\Sigma} \triangleq \text{Diag}\left\{M(Q+1)\mathbf{I}_S, MQ\mathbf{I}_{M-S}\right\}$. We now define $\mathbf{g}_0^{(\mu)} \triangleq \mathbf{F}_M^H\bar{\mathbf{h}}_0^{(\mu)}$, and

$$\mathbf{g}_1^{(\mu)} \triangleq \text{Diag}\left\{\sqrt{Q/(Q+1)}\mathbf{I}_S, \mathbf{I}_{M-S}\right\}\mathbf{g}_0^{(\mu)}, \tag{25}$$

$$\mathbf{g}_2^{(\mu)} \triangleq \text{Diag}\left\{\mathbf{I}_S, \sqrt{(Q+1)/Q}\mathbf{I}_{M-S}\right\}\mathbf{g}_0^{(\mu)}, \tag{26}$$

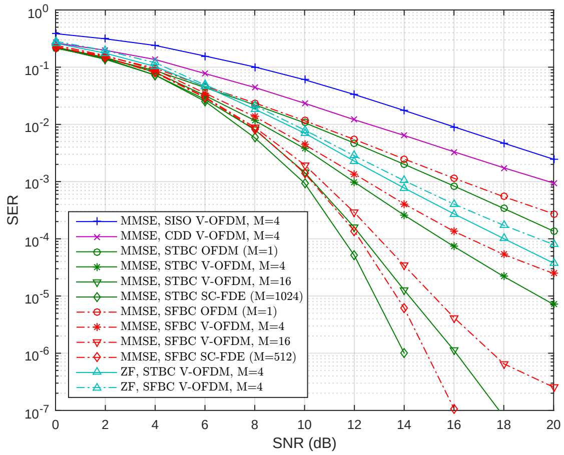

Fig. 4. The performances of V-OFDM systems over time-invariant channels.

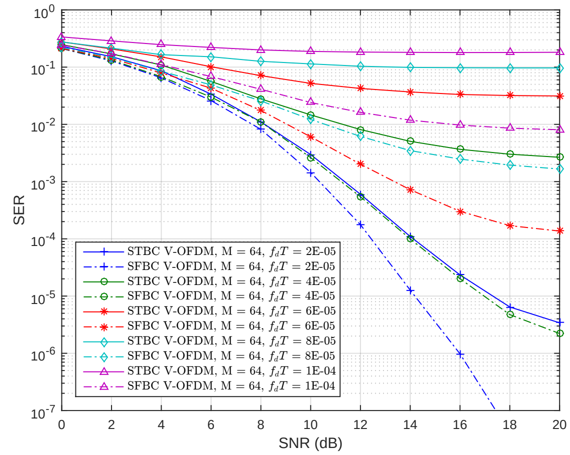

Fig. 5. The performances of V-OFDM systems over time-varying channels.

Also, we define the corresponding probabilities

$$P_p \triangleq \mathbb{P}\left\{\sum_{m=0}^{M-1}\frac{1}{1+\rho\left|\left[\mathbf{g}_p^{(1)}\right]_m\right|^2+\rho\left|\left[\mathbf{g}_p^{(2)}\right]_m\right|^2} > \frac{M}{2^R}\right\}, \quad (27)$$

for $p = 0, 1, 2$. Similar to [3, (23)], we can obtain $P_{\text{out}} \doteq P_0$. Moreover, since $|[\mathbf{g}_1^{(\mu)}]_m|^2 \leq |[\mathbf{g}_0^{(\mu)}]_m|^2 \leq |[\mathbf{g}_2^{(\mu)}]_m|^2$ for any μ and m, we have $P_1 \geq P_0 \geq P_2$. Also, considering that the entries of $\mathbf{g}_1^{(\mu)}$ and $\mathbf{g}_2^{(\mu)}$ are i.i.d. Gaussian random variables, based on Lemma 1, we can get $P_1 = P_2 \doteq \rho^{-2\left(\lfloor M2^{-R}\rfloor+1\right)}$, which brings us back to (23).

Therefore, the diversity order for the case $M < D + 1$ is

$$d^{\text{MMSE}} = 2\left(\lfloor M2^{-R}\rfloor + 1\right). \quad (28)$$

At last, combining (21) and (28), we have the diversity order shown in (18), which concludes our proof. ■

Theorem 2: In 2×1 frequency-selective channels with i.i.d. zero-mean complex Gaussian taps, the diversity order of the STBC V-OFDM system with ZF equalization is $d^{\text{ZF}} = 2$.

In contrast to its MMSE counterpart, the detection SINR of the STBC V-OFDM system with ZF equalization is

$$\gamma_{l,m}^{\text{ZF}} = \left[\frac{1}{\rho M}\text{Tr}\left\{\tilde{\mathbf{H}}_l^{-1}\right\}\right]^{-1}. \quad (29)$$

Based on the analyses in [9, Theorem 4] and [10, IV.B], and following the same procedure as in Theorem 1, it is easy to show that $d^{\text{ZF}} = 2$. The detailed proof is omitted.

Remark 3: Although the discussions here focus on the STBC system, under the Alamouti assumption, the same analyses can also be applied to the SFBC V-OFDM system. Besides, the latter may have a better performance over time-varying channels, which is shown in the next section.

IV. Simulation Results

The symbol error rate (SER) performances of the 1×1 SISO, 2×1 CDD, STBC and SFBC V-OFDM systems are evaluated over time-invariant channels in Fig. 4, where QPSK is adopted, i.e., $R = 2$ and the channel memory length is set to $D = 32$. It can be seen that the proposed STBC and SFBC V-OFDM systems outperform their SISO and CDD counterparts, and MMSE equalization always has a better performance than ZF equalization. Moreover, the SER slope of the MMSE V-OFDM system increases with M. Also, as special cases of the V-OFDM system, STBC (SFBC) OFDM and SC-FDE provide two extreme diversity orders. These observations verify the theoretical analysis in Section III.

Meanwhile, with the limitation of coherence bandwidth, the Alamouti assumption of space-frequency coding is not precisely held, which causes the SFBC systems to have an inferior performance compared to the STBC ones. However, as shown in Fig. 5, over time-varying channels with a moderate normalized Doppler frequency f_dT, where T is the symbol duration, the STBC system exhibits obvious error floors, while the SFBC system offers a better resilience to time variations.

References

[1] X.-G. Xia, "Precoded vector OFDM robust to channel spectral nulls and with reduced cyclic prefix length in single transmit antenna systems," *IEEE Trans. Commun.*, vol. 49, no. 8, pp. 1363–1374, Aug. 2001.

[2] P. Cheng, M. Tao, Y. Xiao, and W. Zhang, "V-OFDM: On performance limits over multi-path rayleigh fading channels," *IEEE Trans. Commun.*, vol. 59, no. 7, pp. 1878–1892, Jul. 2011.

[3] Y. Li, I. Ngebani, X.-G. Xia, and A. Host-Madsen, "On performance of vector OFDM with linear receivers," *IEEE Trans. Signal Process.*, vol. 60, no. 10, pp. 5268–5280, Oct. 2012.

[4] W. Han, X.-G. Xia, and J.-H. Ge, "Cyclic delay transmission for vector OFDM systems," *IEEE Trans. Wireless Commun.*, submitted.

[5] K. Lee and D. Williams, "A space-time coded transmitter diversity technique for frequency selective fading channels," in *Proc. IEEE SAM Signal Process. Workshop*, Mar. 2000, pp. 149–152.

[6] N. Al-Dhahir, "Single-carrier frequency-domain equalization for space-time block-coded transmissions over frequency-selective fading channels," *IEEE Commun. Lett.*, vol. 5, no. 7, pp. 304–306, Jul. 2001.

[7] K. Lee and D. Williams, "A space-frequency transmitter diversity technique for OFDM systems," in *Proc. IEEE Global Telecommun. Conf.*, vol. 3, Dec. 2000, pp. 1473–1477.

[8] J.-H. Jang, H.-C. Won, and G.-H. Im, "Cyclic prefixed single carrier transmission with SFBC over mobile wireless channels," *IEEE Signal Process. Lett.*, vol. 13, no. 5, pp. 261–264, May 2006.

[9] A. Tajer and A. Nosratinia, "Diversity order in ISI channels with single-carrier frequency-domain equalizers," *IEEE Trans. Wireless Commun.*, vol. 9, no. 3, pp. 1022–1032, Mar. 2010.

[10] A. Mehana and A. Nosratinia, "Single-carrier frequency-domain equalizer with multi-antenna transmit diversity," *IEEE Trans. Wireless Commun.*, vol. 12, no. 1, pp. 388–397, Jan. 2013.